Simultaneous Conduction and Radiation in a Two-Layer Planar Medium

C.-H. Ho* and M. N. Özisik†
North Carolina State University, Raleigh, North Carolina

The interaction of radiation with conduction is investigated under steady-state conditions for a two-layer, absorbing, emitting, and isotropically scattering slab with a semitransparent interface. The outer boundaries are assumed to be black and are subjected to constant but different temperatures. An analytic approach is applied to solve the radiation part of the problem. A finite difference scheme is used for the solution of the conduction part. The reflectivities on both sides of the interface, and the relative magnitudes of the radiation and conduction properties of the layers, have significant effect on the temperature distribution in the medium, as well as on the proportion of the production and radiation fluxes in the medium. The effects of the conduction-to-radiation parameter, the single scattering albedo, the optical thickness, and the interface reflectivity on the temperature distribution and heat flux are examined.

Nomenclature

$a_{i,n}$	= unknown coefficients in the dimensionless incident radiation
$B_{j,m,n}$, $d_{j,m}$	= elements
$E_n(z)$	= exponential integral function
G_i	= dimensionless incident radiation
H_i	= dimensionless source term
$h_{i,\ell}$	= known coefficients in the dimensionless source term
k_i	= thermal conductivity
L_0	= total thickness of the two-layer slab
N_i	= conduction-to-radiation parameter, $k_i/L_0/4n^2\bar{\sigma}T_{\mathrm{ref}}^3$
n	= refractive index
Q^c	= dimensionless conduction heat flux, $q^c/4n^2\bar{\sigma}T_{\mathrm{ref}}^4$
Q^r	= dimensionless net radiation heat flux, $q^r/4n^2\bar{\sigma}T_{\mathrm{ref}}^4$
Q^t	= dimensionless total heat flux, Q^c+Q^r
q^c,q^r	= conduction and net radiation heat flux, respectively
T_i	= temperature in the layer i
T_{ref}	= reference temperature
x	= spatial coordinate
α	= dimensionless thickness of layer 1
β_i	= extinction coefficient for layer i
Γ_i	= interface transmissivity as viewed from layer i
η	= dimensionless spatial coordinate, x/L_0
μ	= direction cosine
θ_i	= T_i/T_{ref}
ρ_i	= interface reflectivity as viewed from layer i
$\bar{\sigma}$	= Stefan Boltzmann constant
τ	= optical variable
Ψ_i	= dimensionless radiation intensity
ω_i	= single scattering albedo

Subscript

i	= 1 or 2, referring to the first and second layer, respectively

Received March 10, 1986; revision received May 15, 1986.

*Graduate Student, Mechanical and Aerospace Engineering Department.
†Professor, Mechanical and Aerospace Engineering Department.

Introduction

A VAST amount of work is available in the literature on simultaneous conduction and radiation for a single-layer participating medium.[1-6] For the case of a two-layer slab, some solutions are given for the problem of pure radiation[7,8]; but, to our knowledge, no work appears on combined conduction and radiation, despite the fact that such problems have numerous important applications in a variety of areas, including heat transfer through porous insulation layers, semitransparent materials and various fibrous and foam insulations, plastics, and paints. The analysis of such problems is complicated by the coupling of the equations of radiative transfer and heat conduction. Therefore, the objective of this work is to present the effects of various parameters on the temperature distribution and heat flow in simultaneous conduction and radiation through a two-layer, planar, semitransparent medium confined between two black outer boundaries.

Analysis

Consider one-dimensional, steady-state, combined conduction and radiation heat transfer in a two-layer absorbing, emitting, isotropically scattering, constant property slab subjected to a constant temperature at the outer surfaces. It is assumed that the interface between the layers reflects and transmits radiation, but does not absorb or emit radiation. The mathematical formulation of this problem, in the dimensionless form, is

$$\frac{\mathrm{d}^2\theta_i}{\mathrm{d}\eta^2}=\frac{1}{N_i}\frac{\mathrm{d}Q_i^r}{\mathrm{d}\eta},\qquad \text{in } 0<\eta<\alpha,\quad i=1$$

$$\text{and } \alpha<\eta<1,\quad i=2 \tag{1a}$$

with the boundary conditions

$$\theta_1=\theta_L \qquad \text{at } \eta=0 \quad \text{(left boundary)} \tag{1b}$$

$$\theta_1=\theta_2 \qquad \text{at } \eta=\alpha \quad \text{(interface)} \tag{1c}$$

$$N_1\frac{\mathrm{d}\theta_1}{\mathrm{d}\eta}=N_2\frac{\mathrm{d}\theta_2}{\mathrm{d}\eta} \qquad \text{at } \eta=\alpha \quad \text{(interface)} \tag{1d}$$

$$\theta_2=\theta_R \qquad \text{at } \eta=1 \quad \text{(right boundary)} \tag{1e}$$

Where various quantities are defined as

$$\theta_i = T_i/T_{\text{ref}} = \text{dimensionless temperature}, \; i=1,2 \qquad (2a)$$

$$N_i = (k_i/L_0)/4n^2\bar{\sigma}T_{\text{ref}}^3 = \text{conduction-to-radiation parameter} \quad i=1,2 \qquad (2b)$$

$$Q_i^r = (q_i^r)/(4n^2\bar{\sigma}T_{\text{ref}}^4) = \text{dimensionless net radiation heat flux} \quad i=1,2 \qquad (2c)$$

$$\eta = x/L_0 = \text{dimensionless coordinate} \qquad (2d)$$

$$L_0 = \text{total thickness of the two layers} \qquad (2e)$$

$$\alpha = \text{dimensionless thickness of layer 1} \qquad (2f)$$

The gradient of dimensionless net radiation heat flux, $dQ_i^r/d\eta$, in Eq. (1) can be expressed as[9]

$$\frac{dQ_i^r}{d\eta} = \beta_i L_0 \frac{dQ_i^r}{d\tau} = \beta_i L_0 (1-\omega_i)(\theta_i^4 - G_i), \qquad i=1,2 \qquad (3)$$

where β_i is the extinction coefficient and ω_i the single scattering albedo. The optical thickness τ is defined as

$$\tau = \begin{cases} \beta_1 L_0 \eta & \text{for } 0<\eta<\alpha \\ (\beta_1-\beta_2)L_0\alpha + \beta_2 L_0 \eta & \text{for } \alpha<\eta<1 \end{cases} \qquad (4)$$

and the dimensionless incident radiation $G_i(\tau)$ is related to the dimensionless intensity $\Psi_i(\tau,\mu)$ by

$$G_i(\tau) = \frac{1}{2}\int_{-1}^{1} \Psi_i(\tau,\mu)d\mu, \qquad i=1,2 \qquad (5)$$

Here, $\Psi_i(\tau,\mu)$ satisfies the equation of radiative transfer

$$\mu\frac{d}{d\tau}\Psi_i(\tau,\mu) + \Psi_i(\tau,\mu) = H_i(\tau) + \frac{\omega_i}{2}\int_{-1}^{1}\Psi_i(\tau,\mu')d\mu' \qquad (6a)$$

where $0<\tau<\tau_1$ for $i=1$ and $\tau_1<\tau<\tau_2$ for $i=2$ and μ is the cosine of the angle between the positive τ axis and the direction of the radiation intensity. The dimensionless source term $H_i(\tau)$ is related to the temperature by

$$H_i(\tau) = (1-\omega_i)\theta_i^4(\tau), \qquad i=1,2 \qquad (6b)$$

We assume black outer boundaries and a semitransparent interface which reflects and transmits radiation, but does not absorb and emit it. Then the boundary conditions for the equation of radiative transfer become

$$\Psi_1(0,\mu) = \theta_L^4 \qquad \text{(left boundary)} \qquad (6c)$$

$$\Psi_1(\tau_1,-\lambda) = \rho_1\Psi_1(\tau_1,\mu) + \Gamma_2\Psi_2(\tau_1,-\mu) \qquad \text{(interface)} \qquad (6d)$$

$$\Psi_2(\tau_1,\mu) = \rho_2\Psi_2(\tau_1,-\mu) + \Gamma_1\Psi_1(\tau_1,\mu) \qquad \text{(interface)} \qquad (6e)$$

$$\Psi_2(\tau_2,-\mu) = \theta_R^4 \qquad \text{(right boundary)} \qquad (6f)$$

where ρ_1 and Γ_1 are the interface reflectivity and transmissivity, respectively, when viewed from the first layer; and ρ_2 and Γ_2 are the interface reflectivity and transmissivity, respectively, when viewed from the second layer. We also assume that ρ_i and Γ_i are angular independent and $\rho_i + \Gamma_i = 1.0$ for $i=1,2$.

The condition problem given in Eqs. (1) and the radiation problem defined by Eqs. (6) provide the complete mathematical formulation for the simultaneous conduction and radiation problem. An iterative scheme is needed to solve this system because the energy equation (1a) involves the radiation heat flux, whereas the equation of radiative transfer, Eqs. (6), needs the temperature distribution in the medium. Assuming an initial guess is available for $\theta_i(\eta)$, the radiation problem can be solved by a suitable method. We use the generalization of the Galerkin method[10] to develop a solution for radiation transfer in an absorbing, emitting, isotropically scattering two-layer slab. The general procedure is similar to that given in Ref. 10, but the analysis is more involved. By following the formalism of this approach, we expand the incident radiation $G_i(\eta)$ in a polynomial of order K_i in the powers of τ

$$G_i(\tau) = \sum_{n=0}^{K_i} a_{i,n}\tau^n, \qquad i=1,2 \qquad (7)$$

where a_i,n are the unknown expansion coefficients. We assume the source term $H_i(\eta)$ also can be expressed in a polynomial of order L_i in powers of τ

$$H_i(\tau) = \sum_{\ell=0}^{L_i} h_{i,\ell}\tau^\ell, \qquad i=1,2 \qquad (8)$$

where $h_{i,\ell}$ are the known coefficients.

We apply the Galerkin method to the integral form of the equation of radiative transfer for a two-layer slab. Omitting the details of the analysis on the transformation of the equation of radiative transfer into a system of integral equations for the incident radiation $G_i(\eta)$ and the application of the Galerkin method that reduces this sytem into a set of algebraic equations for the unknown expansion coefficients $a_{i,n}$, we present the resulting system of algebraic equations for the coefficients $a_{i,n}$, in the matrix form

$$\left[\begin{array}{c|c} B_{1,m,n} & B_{2,m,n} \\ \hline B_{3,m,n} & B_{4,m,n} \end{array}\right] \left[\begin{array}{c} a_{1,n} \\ \hline a_{2,n} \end{array}\right] = \left[\begin{array}{c} d_{1,m} \\ \hline d_{2,m} \end{array}\right] \qquad (9)$$

elements $B_{j,m,n}$, $j=1,2,3,4$, and $d_{j,m}$, $j=1,2$ are listed in Appendix A.

Once the expansion coefficients $a_{i,n}$ are determined from the solution of Eqs. (9), the net radiation heat flux anywhere in the medium is obtained from

$$\begin{aligned} Q_1^r(\tau) = 2\pi\Bigg\{&\theta_L^4 E_3(\tau) - I_1(\tau) + \sum_{\ell=0}^{L_1} h_{1,\ell}\ell!\Bigg[(-1)^{\ell+1}E_{\ell+3}(\tau) \\ &+ \sum_{i=0}^{\ell}\left[\frac{(-1)^i\tau^{\ell-i}}{(\ell-i)!(i+2)} + \frac{1}{(\ell-i)!}\left(\tau_1^{\ell-i}E_{i+3}(\tau_1-\tau) - \frac{\tau^{\ell-i}}{(i+2)}\right)\right]\Bigg] \\ &+ \frac{\omega_1}{4\pi}\sum_{n=0}^{K_1} a_{1,n}n!\Bigg[(-1)^{n+1}E_{n+3}(\tau) + \sum_{i=0}^{n}\Bigg[\frac{(-1)^i\tau^{n-i}}{(n-i)!(i+2)} \\ &+ \frac{1}{(n-i)!}\left(\tau_1^{n-i}E_{i+3}(\tau_1-\tau) - \frac{\tau^{n-i}}{(i+2)}\right)\Bigg]\Bigg]\Bigg\} \end{aligned} \qquad (10a)$$

for region 1, and

$$\begin{aligned} Q_2^r(\tau) = 2\pi\Bigg\{&\theta_R^4 E_3(\tau_2-\tau) + I_2(\tau) \\ &+ \sum_{\ell=0}^{L_2} h_{2,\ell}\ell!\sum_{i=0}^{\ell}\left[\frac{(-1)^i}{(\ell-i)!}\left(\frac{\tau^{\ell-i}}{(i+2)} - \tau_1^{\ell-i}E_{i+3}(\tau-\tau_1)\right)\right. \\ &\left.+ \frac{1}{(\ell-i)!}\left(\tau_2^{\ell-i}E_{i+3}(\tau_2-\tau) - \frac{\tau^{\ell-i}}{(i+2)}\right)\right] - \frac{\omega_2}{4\pi}\sum_{n=0}^{K_2} a_{2,n}n! \\ &\times \sum_{i=0}^{n}\left[\frac{(-1)^i}{(n-i)!}\left(\frac{\tau^{n-i}}{i+2} - \tau_1^{n-i}E_{i+3}(\tau-\tau_1)\right)\right. \\ &\left.+ \frac{1}{(n-i)!}\left(\tau_2^{n-i}E_{i+3}(\tau_2-\tau) - \frac{\tau^{n-i}}{i+2}\right)\right]\Bigg\} \end{aligned} \qquad (10b)$$

for region 2. Here the $E_n(z)$ are the exponential integral functions, and $I_1(\tau)$ and $I_2(\tau)$ are the integrals for which explicit analytical expressions are given in Appendix B.

Clearly, given the boundary temperatures θ_L and θ_R, the optical thickness, and the single scattering albedo for each layer, and specifying the interface reflectivity, transmissivity, and the expansion coefficients $h_{i,\ell}$ for the source term $H_i(\tau)$, the net radiation heat flux is readily determined anywhere in the medium from Eqs. (10) because the unknown expansion coefficients $a_{i,n}$ are available from the solution of Eqs. (9).

Once $a_{i,n}$ are available the incident radiation $G_i(\tau)$ is computed from the expansion coefficients $a_{i,n}$. The divergence of the radiation heat flux vector $dQ_i^r/d\eta$ is determined from Eq. (3). With the availability of $dQ_i^r/d\eta$, the energy equation of Eqs. (1) is solved by using a finite difference scheme, by dividing each layer into J_i+1 intervals. Then the heat conduction problem of Eqs. (1) is transferred into the following system of algebraic equations

$$\theta_{i,j-1}-2\theta_{i,j}+\theta_{i,j+1} = A_i(\theta_{i,j}^4-G_{i,j}) \quad \begin{cases} i=1,2 \text{ for region 1 and 2} \\ j=1,2,\ldots,J_i \text{ for the nodes} \end{cases} \tag{11a}$$

$$\theta_{1,0}=\theta_L \tag{11b}$$

$$\theta_{1,J_1+1}=\theta_{2,0} \tag{11c}$$

$$N_1(\theta_{1,J_1}-\theta_{1,J_1}+1)/(\Delta\eta_1)=N_2(\theta_{2,0}-\theta_{2,1})/(\Delta\eta_2) \tag{11d}$$

$$\theta_{2,J_2}+1=\theta_R \tag{11e}$$

where the parameter A_i is defined as

$$A_i=\Delta\eta_i^2[\beta_i L_0(1-\omega_i)]/N_i \qquad i=1,2 \tag{12}$$

with the $\Delta\eta_i$ being the mesh size. The solution of Eqs. (11) yields the temperature distribution $\theta_{i,j}$ in the medium.

An iterative scheme was used to solve the energy problem of Eqs. (11), together with the transformed radiation problem given by Eqs. (9). The number of iterations needed for convergence depended on the radiation properties of the layers. In general, more iterations were needed with increasing optical thickness τ_i or decreasing conduction-to-radiation parameter N_i. For a conduction-to-radiation parameter of less than about 0.5, some oscillations were observed in θ_i, and the solution diverged for N_i less than 0.1. To overcome this difficulty, an underrelaxation factor was applied to the iterations for temperature. Then the results converged without any difficulty.

Special cases of current analysis were compared with those already available in the literature to validate the present work. Comparisons made for the case of combined conduction and radiation in a single-layer slab with reported works,[2,6] and for the case of pure radiation in a two-layer slab with Ref. 8 showed agreement to three decimal digits.

Results and Discussion

We now present numerical results to illustrate the effects of various parameters on simultaneous conduction and radiation in a two-layer slab with black outer boundaries maintained at constant but different temperatures. The refractive indices of each medium in a two-layer slab are generally not the same. As a result, some reflection occurs at the interface. However, for the cases aimed at illustrating the effects of other parameters, such as the conduction-to-radiation parameter, optical thickness, and the single scattering albedo for the layers, a parameter survey was made by assuming a transparent interface. Later on, we investigated separately the effects of interface reflectivities.

Consider the situation in which both layers have equal optical thicknesses, $\tau_1=\tau_2=1.5$, and the boundary surfaces at $\eta=0$ and $\eta=1$ are kept at temperatures $\theta=0.5$ and $\theta=1.0$, respectively. The effects of a single scattering albedo are examined by considering the two extreme values $\omega=0$ and $\omega=1$, respectively, corresponding to purely absorbing and purely scattering medium. Two different values of the conduction-to-radiation parameter chosen included $N=1$ and $N=0.01$, representing the conduction dominant and the radiation dominant cases, respectively. Figure 1 shows that when conduction is dominant (i.e., $N=1$) in any one of the layers, the variation of albedo from $\omega=0$ to $\omega=1$ has a small effect on the temperature distribution θ in that layer. The reason is that in

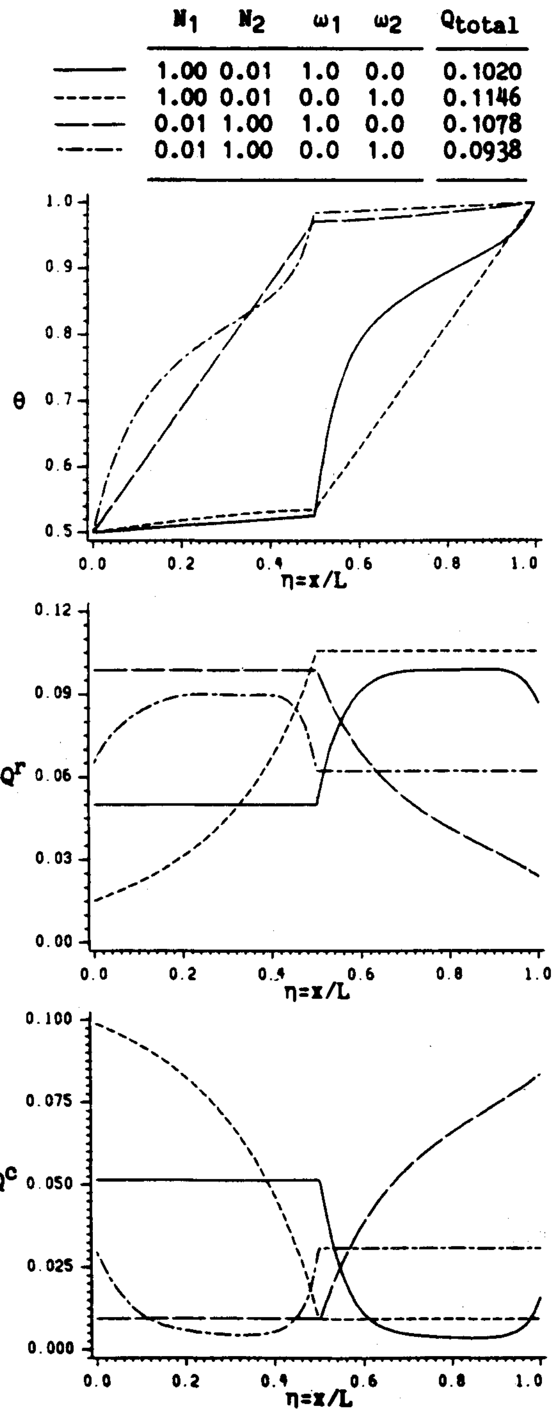

Fig. 1 Effects of the conduction-to-radiation parameters and the single scattering albedo on the temperature distribution and heat flux for $\tau_1=\tau_2=1.5$, $\rho_1=\rho_2=0.0$, $\theta_L=0.5$, and $\theta_R=1.0$.

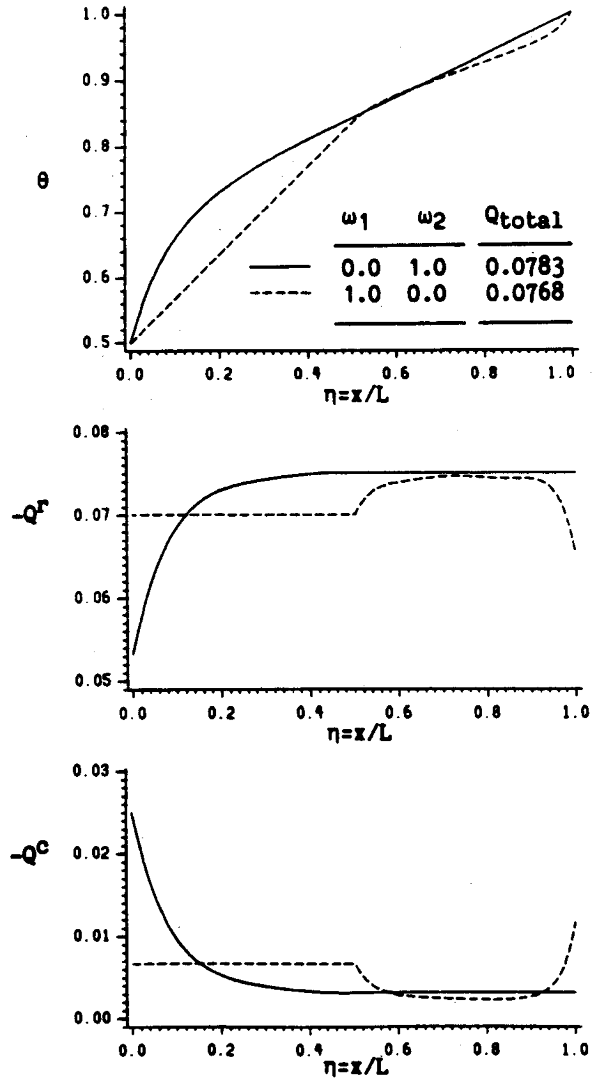

Fig. 2 Effects of the single scattering albedo, ω_1 and ω_2, on the temperature distribution and heat flux for $N_1 = N_2 = 0.01$, $\tau_1 = \tau_1 = 1.5$, $\rho_1 = \rho_2 = 0.0$, $\theta_L = 0.5$, and $\theta_R = 1.0$.

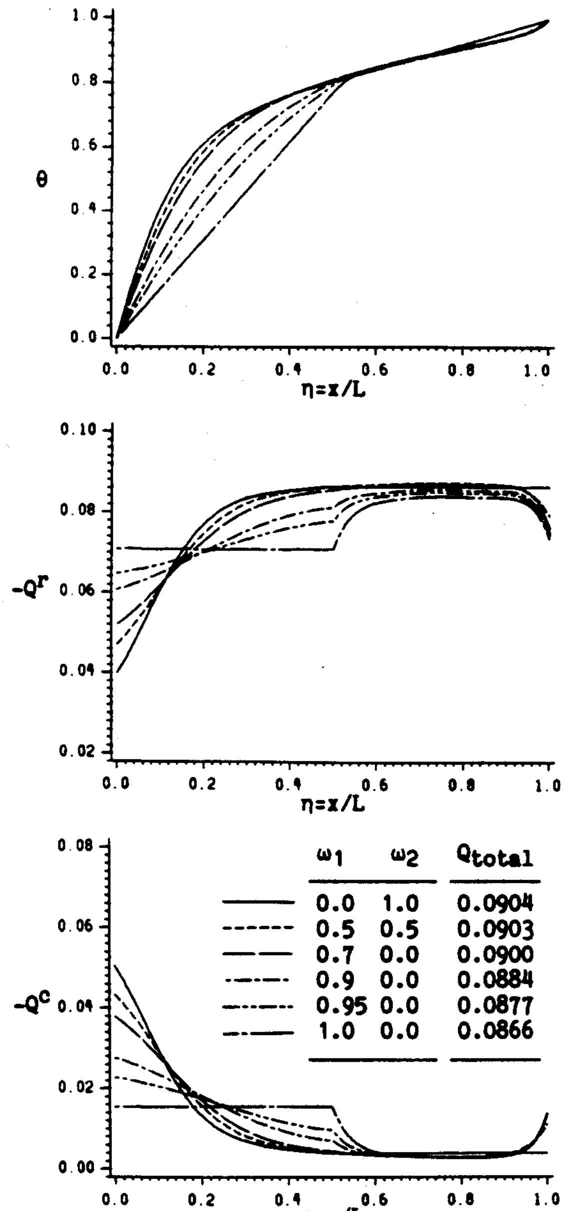

Fig. 3 Effects of the single scattering albedo, ω_1 and ω_2, on the temperature distribution and heat flux for $N_1 = N_2 = 0.01$, $\tau_1 = \tau_2 = 1.5$, $\rho_1 = \rho_2 = 0.0$, $\theta_L = 0.0$, and $\theta_R = 1.0$.

the conduction dominant layer, a greater proportion of heat transfer is by conduction. Hence, any change in the radiation flux resulting from the variation of ω does not significantly affect the temperature profile. Note that the temperature profile for the case $\omega = 1$ is identical to that for pure conduction because the conduction and radiation are uncoupled for $\omega = 1$. The distribution of the conduction and radiation fluxes in the medium and the values of the total heat flux $Q^t = Q^c + Q^r$ for each of the four different cases considered are also presented in Fig. 1. For the case $\omega = 1$, both the conduction and radiation fluxes remain constant in the medium because of the uncoupling of conduction and radiation problems. An examination of the temperature profiles in Fig. 1 reveals that the slope of temperature is much less for the conduction dominant layer than the radiation dominant layer. Therefore, the temperature distribution over the medium becomes lower when the radiation dominant layer is adjacent to the high temperature boundary.

In Fig. 2, the values of the conduction-to-radiation parameters are fixed as $N_1 = N_2 = 0.01$, the optical thicknesses are taken as $\tau_1 = \tau_2 = 1.5$, and the boundary surfaces $\eta = 0$ and $\eta = 1$ are maintained at $\theta = 0.5$ and $\theta = 1.0$, respectively. For this radiation dominant case, the effects of a single scattering albedo are examined by considering the limiting combinations $\omega_1 = 0$, $\omega_2 = 1$ and $\omega_1 = 1$, $\omega_2 = 0$. The results, presented in Fig. 2, show that the temperature of the layer adjacent to the low-temperature boundary is affected more by the variation of ω than that of the layer next to the high-temperature boundary. The case when both layers are purely absorbing ($\omega_1 = \omega_2 = 0$) is not included in the results of Fig. 2 because the resulting temperature profile followed the curve for $\omega_1 = 0$ in the first layer, then moved smoothly to the curve for $\omega_2 = 0$ in the second layer, and then closely followed it. The total heat flux for the case $\omega_1 = \omega_2 = 0$ was 0.0796, which was higher than that shown in Fig. 2.

Figure 3 shows the effect of ω_1 and ω_2 on temperature distribution and heat fluxes for the case $\tau_1 = \tau_2 = 1.5$ and $N_1 = N_2 = 0.01$ when the boundary surface temperature at $\eta = 0$ is reduced to $\theta = 0$. As expected, the radiation effects become more pronounced for the case with $\theta = 0$ at $\eta = 0$ and $\theta = 1$ at $\eta = 1$. This figure shows results for several different combinations of ω_1 and ω_2. Note that the temperature profiles for the intermediate values of ω_1 and ω_2 lie between those for the two limiting cases of $\omega_1 = 0$, $\omega_2 = 1$ and $\omega_1 = 1$, $\omega_2 = 0$.

Figure 4 shows the effects of the optical thickness variation of the layers on the temperature distribution when the total

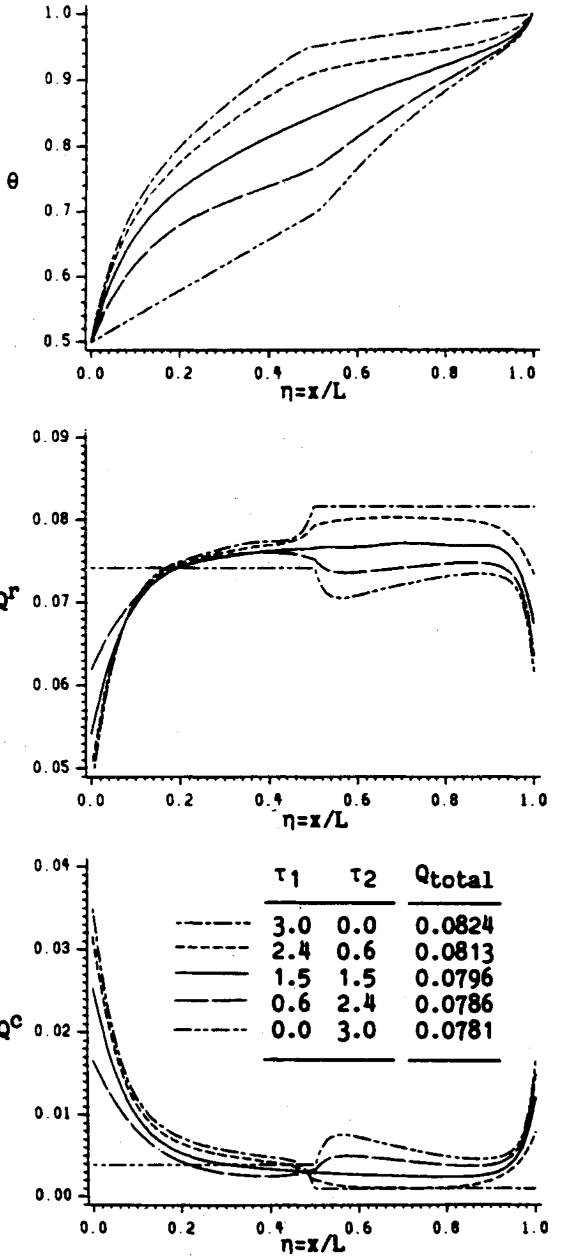

Fig. 4 Effects of the optical thicknesses, τ_1 and τ_2, on the temperature distribution and heat flux for $N_1 = N_2 = 0.01$, $\omega_1 = \omega_2 = 0.0$, $\rho_1 = \rho_2 = 0.0$, $\theta_L = 0.5$, and $\theta_R = 1.0$.

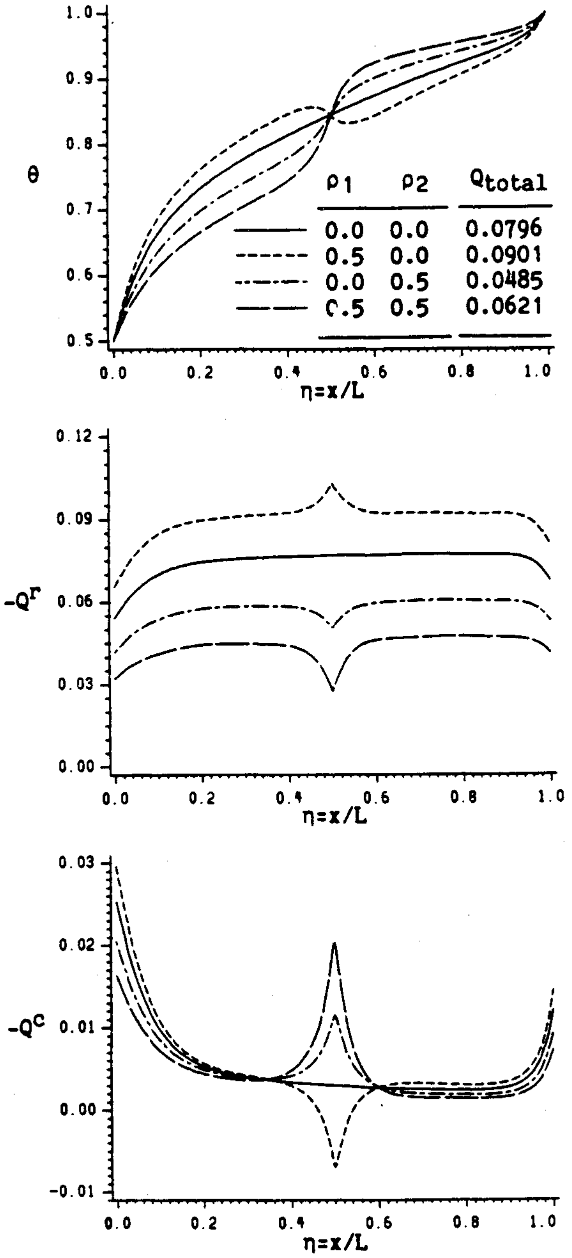

Fig. 5 Effects of the interface reflectivities, ρ_1 and ρ_2, on the temperature distribution and heat flux for $N_1 = N_2 = 0.01$, $\tau_1 = \tau_2 = 1.5$, $\omega_1 = \omega_2 = 0.0$, $\theta_L = 0.5$, and $\theta_R = 1.0$.

optical thickness is kept at $\tau_1 + \tau_2 = 3$. Other parameters are fixed at $N_1 = N_1 = 0.01$, $\omega_1 = \omega B_2 = 0$. By varying τ_1 and τ_2, five different combinations of the optical thickness are considered. The two limiting cases, $\tau_1 = 0$ ($\tau_2 = 3$) and $\tau_1 = 3$ ($\tau_2 = 0$), correspond to a transparent first and second layer, respectively. When the layer next to the hot boundary is transparent, the temperature of the medium is highest. Conversely, when the layer next to the cold surface is transparent, the temperature of the medium is lowest. Temperatures for all other combinations lie between these two limiting cases.

Figure 5 shows the effect of the interface reflectivities, ρ_1 and ρ_2, on the temperature distribution, net radiative heat flux, and conductive heat flux for the cases of $N_1 = N_2 = 0.01$, $\tau_1 = \tau_2 = 1.5$, and $\omega_1 = \omega_2 = 0$. The case $\rho_1 = 0.5$ and $\rho_2 = 0.0$ corresponds to an interface that is transparent when viewed from the second layer, while the case $\rho_1 = 0$ and $\rho_2 = 0.5$ represents an interface, that is transparent when viewed from the first layer. The highest and lowest radiation fluxes occur, respectively with the cases $\rho_1 = 0.5$, $\rho_2 = 0.0$ and $\rho_1 = 0.0$, $\rho_2 = 0.5$. Since the radiation flux is in the negative τ direction, any increase in the value of ρ_2 at the interface reflects the radiation back, hence reducing the radiation flux. For purposes of comparison, heat transfer results are given for both a completely transparent interface ($\rho_1 = \rho_2 = 0$) and an interface which has some reflectivity at both sides ($\rho_1 = \rho_2 = 0.5$).

The dimensionless temperatures and heat fluxes are presented in Tables 1 and 2, respectively, at several different locations, for various combinations of optical thicknesses, single scattering albedo, and conduction-to-radiation parameters for the case $\tau_1 + \tau_2 = 3.0$. The effects of optical thickness and single scattering albedo are more pronounced for small values of N_1 and N_2; that is, when radiation is dominant. For given values of N_1, N_2, ω_1, and ω_2, the total heat flux is maximum when τ_1 is largest.

All numerical computations were performed with an IBM 4341 computer. The CPU time required to produce each case in Tables 1 and 2 varied from about 2 min, for $N = 1$, to about 12 min, for $N = 0.01$.

Table 1 Dimensionless temperature at different locations for various combinations of N_1, N_2, τ_1, τ_2, ω_1, and ω_2 with $\rho_1=\rho_2=0.0$, $\theta_L=0.5$, and $\theta_R=1.0$

					Temperature θ		
$N_1=N_2$	τ_1	τ_2	ω_1	ω_2	$\eta=0.25$	0.50	0.75
			0	0	0.6402	0.7693	0.8849
	2.4	0.6	0	0.95	0.6393	0.7672	0.8836
			0.95	0	0.6321	0.7613	0.8828
			0	0	0.6336	0.7599	0.8801
1.0	1.5	1.5	0	0.95	0.6328	0.7581	0.8790
			0.95	0	0.6295	0.7577	0.8802
			0	0	0.6278	0.7519	0.8758
	0.6	2.4	0	0.95	0.6276	0.7517	0.8757
			0.95	0	0.6261	0.7518	0.8762
			0	0	0.7169	0.8521	0.9219
	2.4	0.6	0	0.95	0.7137	0.8460	0.9224
			0.95	0	0.6743	0.8224	0.9182
			0	0	0.6824	0.8053	0.8990
0.1	1.5	1.5	0	0.95	0.6794	0.7998	0.8987
			0.95	0	0.6540	0.7958	0.9008
			0	0	0.6464	0.7603	0.8781
	0.6	2.4	0	0.95	0.6454	0.7611	0.8787
			0.95	0	0.6316	0.7596	0.8803
			0	0	0.8023	0.9097	0.9409
	2.4	0.6	0	0.95	0.8006	0.9065	0.9469
			0.95	0	0.7693	0.9029	0.9427
			0	0	0.7556	0.8440	0.9103
0.01	1.5	1.5	0	0.95	0.7535	0.8410	0.9114
			0.95	0	0.7140	0.8430	0.9130
			0	0	0.6957	0.7650	0.8790
	0.6	2.4	0	0.95	0.6937	0.7679	0.8763
			0.95	0	0.6489	0.7664	0.8815

Table 2 Dimensionless heat fluxes at different locations for various combinations of N_1, N_2, τ_1, τ_2, ω_1, and ω_2 with $\rho_1=\rho_2=0.0$, $\theta_L=0.5$, and $\theta_R=1.0$

					Radiation heat flux Q^r			Conduction heat flux Q^c			Total flux
$N_1=N_2$	τ_1	τ_2	ω_1	ω_2	$\eta=0.25$	0.5	0.75	$\eta=0.25$	0.5	0.75	$Q^t=Q^r-Q^c$
			0	0	0.0190	0.1196	0.1181	0.5757	0.4751	0.4766	0.5947
	2.4	0.6	0	0.95	0.0188	0.1244	0.1244	0.5722	0.4666	0.4666	0.5910
			0.95	0	0.0499	0.0719	0.1015	0.5322	0.5102	0.4806	0.5821
			0	0	0.0289	0.0862	0.0768	0.5490	0.4917	0.5011	0.5779
1.0	1.5	1.5	0	0.95	0.0291	0.0907	0.0897	0.5463	0.4847	0.4857	0.5754
			0.95	0	0.0533	0.0623	0.0742	0.5200	0.5110	0.4991	0.5733
			0	0	0.0527	0.0803	0.0567	0.5222	0.4946	0.5182	0.5749
	0.6	2.4	0	0.95	0.0513	0.0766	0.0725	0.5209	0.4956	0.4997	0.5722
			0.95	0	0.0670	0.0696	0.0560	0.5052	0.5026	0.5162	0.5722
			0	0	0.0294	0.1034	0.0932	0.1074	0.0334	0.0436	0.1368
	2.4	0.6	0	0.95	0.0287	0.1035	0.1024	0.1057	0.0309	0.0320	0.1344
			0.95	0	0.0554	0.0754	0.0860	0.0738	0.0538	0.0432	0.1292
			0	0	0.0374	0.0859	0.0700	0.0902	0.0417	0.0576	0.1276
0.1	1.5	1.5	0	0.95	0.0366	0.0853	0.0829	0.0886	0.0399	0.0423	0.1252
			0.95	0	0.0596	0.0686	0.0675	0.0639	0.0549	0.0560	0.1235
			0	0	0.0555	0.0802	0.0580	0.0695	0.0448	0.0670	0.1250
	0.6	2.4	0	0.95	0.0538	0.0760	0.0716	0.0687	0.0465	0.0509	0.1225
			0.95	0	0.0691	0.0717	0.0568	0.0535	0.0509	0.0658	0.1226
			0	0	0.0498	0.0793	0.0734	0.0315	0.0020	0.0079	0.0813
	2.4	0.6	0	0.95	0.0492	0.0789	0.0777	0.0313	0.0016	0.0028	0.0805
			0.95	0	0.0643	0.0750	0.0711	0.0144	0.0037	0.0076	0.0787
			0	0	0.0543	0.0766	0.0675	0.0253	0.0030	0.0121	0.0796
0.01	1.5	1.5	0	0.95	0.0535	0.0758	0.0737	0.0251	0.0028	0.0049	0.0786
			0.95	0	0.0667	0.0732	0.0657	0.0108	0.0043	0.0118	0.0775
			0	0	0.0620	0.0753	0.0636	0.0166	0.0033	0.0150	0.0786
	0.6	2.4	0	0.95	0.0610	0.0733	0.0707	0.0164	0.0041	0.0067	0.0774
			0.95	0	0.0704	0.0727	0.0625	0.0068	0.0045	0.0147	0.0772

Appendix A: Elements of the Matrix Equation (9)

$$d_{1,m}=2\pi\Big\{\theta_L^4 m!\Big[\Big(\frac{1}{m+2}-\sum_{j=0}^{m}\frac{\tau_1^{m-j}}{(m-j)!}E_{j+3}(\tau_1)\Big)+\rho_1\Big((-1)^{m+1}E_{m+3}(2\tau_1)-\sum_{j=0}^{m}\frac{\tau_1^{m-j}}{(m-j)!}(-1)^{j+1}E_{j+3}(\tau_1)\Big)\Big]$$
$$+\theta_R^4\Gamma_2 m!\Big[(-1)^{m+1}E_{m+3}(\tau_2)-\sum_{j=0}^{m}\frac{\tau_1^{m-j}}{(m-j)!}(-1)^{j+1}E_{j+3}(\tau_2-\tau_1)\Big]+\sum_{\ell=0}^{L_1}h_{1,\ell}[P_{m,\ell}+T_{m,\ell}]+\sum_{\ell=0}^{L_2}h_{2,\ell}U_{m,\ell}\Big\} \tag{A1}$$

$$d_{2,m}=2\pi\Big\{\theta_L^4\Gamma_1\sum_{j=0}^{m}\frac{m!}{(m-j)!}[\tau_1^{m-j}E_{j+3}(\tau_1)-\tau_2^{m-j}E_{j+3}(\tau_2)]+\theta_R^4 m!\Big[\rho_2\sum_{j=0}^{m}\frac{1}{(m-j)!}\Big(\tau_1^{m-j}E_{j+3}(\tau_2-\tau_1)-\tau_2^{m-j}E_{j+3}(2\tau_2-2\tau_1)\Big)$$
$$+\sum_{j=0}^{m}\frac{(-1)^{j+1}}{(m-j)!}\Big(\tau_1^{m-j}E_{j+3}(\tau_2-\tau_1)-\frac{\tau_2^{m-j}}{j+2}\Big)\Big]+\sum_{\ell=0}^{L_1}h_{1,\ell}V_{m,\ell}+\sum_{\ell=0}^{L_2}h_{2,\ell}[Q_{m,\ell}+R_{m,\ell}]\Big\} \tag{A2}$$

$$B_{1,m,n}=\frac{\tau_1^{n+m+1}}{n+m+1}-\frac{\omega_1}{2}[P_{m,n}+T_{m,n}] \tag{A3}$$

$$B_{2,m,n}=-\frac{\omega_2}{2}U_{m,n} \tag{A4}$$

$$B_{3,m,n}=-\frac{\omega_1}{2}V_{m,n} \tag{A5}$$

$$B_{4,m,n}=\frac{\tau_2^{n+m+1}-\tau_1^{n+m+1}}{n+m+1}-\frac{\omega_2}{2}[Q_{m,n}+R_{m,n}] \tag{A6}$$

where

$$P_{m,n}=\rho_1 n!m!\Big[(-1)^{n+m}E_{n+m+3}(2\tau_1)+\sum_{i=0}^{n}\frac{(-1)^{m+i+1}}{(n-i)!}\tau_1^{n-i}E_{m+i+3}(\tau_1)$$
$$+\sum_{j=0}^{m}\frac{(-1)^{n+j+1}}{(m-j)!}\tau_1^{m-j}E_{n+j+3}(\tau_1)+\sum_{i=0}^{n}\sum_{j=0}^{m}\frac{(-1)^{i+j}}{(n-i)!(m-j)!}\frac{\tau_1^{n+m-i-j}}{(i+j+2)}\Big] \tag{A7}$$

$$T_{m,n}=(-1)^{n+1}\frac{n!m!}{n+m+2}+n!m!\Big[(-1)^n\sum_{j=0}^{m}\frac{\tau_1^{m-j}}{(m-j)!}E_{n+j+3}(\tau_1)+(-1)^m\sum_{i=0}^{n}\frac{\tau_1^{n-i}}{(n-i)!}E_{m+i+3}(\tau_1)\Big]$$
$$+\sum_{i=0}^{n}\frac{n!}{(n-i)!}\frac{[1+(-1)^i]}{i+1}\frac{\tau_1^{m+n-i+1}}{m+n-i+1}-\sum_{i=0}^{n}\sum_{j=0}^{m}\frac{n!m!}{(n-i)!(m-j)!}\times\frac{(-1)^j}{(i+j+2)}\tau_1^{m+n-i-j} \tag{A8}$$

$$U_{m,n}=\Gamma_2 m!n!\Big[\sum_{i=0}^{n}\sum_{j=0}^{m}\frac{(-1)^j\tau_1^{m-j}}{(n-i)!(m-j)!}\Big(\frac{\tau_1^{n-i}}{i+j+2}-\tau_2^{n-i}E_{i+j+3}(\tau_2-\tau_1)\Big)+\sum_{i=0}^{n}\frac{(-1)^{m+1}}{(n-i)!}\Big(\tau_1^{n-i}E_{m+i+3}(\tau_1)-\tau_2^{n-i}E_{m+i+3}(\tau_2)\Big)\Big] \tag{A9}$$

$$V_{m,n}=\Gamma_1 m!n!\Big[\sum_{i=0}^{n}\sum_{j=0}^{m}\frac{(-1)^i\tau_1^{n-i}}{(n-i)!(m-j)!}\Big(\frac{\tau_1^{m-j}}{i+j+2}-\tau_2^{m-j}E_{i+j+3}(\tau_2-\tau_1)\Big)$$
$$+\sum_{j=0}^{m}\frac{(-1)^{n+1}}{(m-j)!}\Big(\tau_1^{m-j}E_{n+j+3}(\tau_1)-\tau_2^{m-j}E_{n+j+3}(\tau_2)\Big)\Big] \tag{A10}$$

$$Q_{m,n}=\rho_2 n!m!\sum_{i=0}^{n}\sum_{j=0}^{m}\Big[\frac{\tau_1^{n+m-i-j}}{(n-i)!(m-j)!}\frac{1}{i+j+2}+\frac{\tau_2^{n+m-i-j}}{(n-i)!(m-j)!}E_{i+j+3}(2\tau_2-2\tau_1)-\frac{\tau_1^{n-i}\tau_2^{m-j}+\tau_2^{n-i}\tau_1^{m-j}}{(n-i)!(m-j)!}E_{i+j+3}(\tau_2-\tau_1)\Big] \tag{A11}$$

$$R_{m,n}=\sum_{i=0}^{n}\frac{n!}{(n-i)!}\frac{[1+(-1)^i]}{i+1}\frac{\tau_2^{n+m-i+1}-\tau_1^{n+m-i+1}}{n+m-i+1}+\sum_{i=0}^{n}\sum_{j=0}^{m}\frac{n!m!}{(n-i)!(m-j)!}\Big\{\frac{1}{i+j+2}\Big[\frac{\tau_1^{n+m-i-j}}{(-1)^{i+1}}+\frac{\tau_2^{n+m-i-j}}{(-1)^{j+1}}\Big]$$
$$-E_{i+j+3}(\tau_2-\tau_1)\Big[\frac{\tau_1^{m-j}\tau_2^{n-i}}{(-1)^{j+1}}+\frac{\tau_1^{n-i}\tau_2^{m-j}}{(-1)^{i+1}}\Big]\Big\} \tag{A12}$$

Appendix B: Analytic Expressions of Integrals $I_1(\tau)$ and $I_2(\tau)$ in Equations (10)

$$
\begin{aligned}
I_1(\tau) = {} & \rho_1 \theta_L^4 E_3(2\tau_1 - \tau) + \Gamma_2 \theta_R^4 E_3(\tau_2 - \tau) + \rho_1 \sum_{\ell=0}^{L_1} h_{1,\ell}\ell! \left[(-1)^{\ell+1} E_{\ell+3}(2\tau_1 - \tau) + \sum_{i=0}^{\ell} \frac{(-1)^i \tau_1^{\ell-i}}{(\ell-i)!} E_{i+3}(\tau_1 - \tau) \right] \\
& + \Gamma_2 \sum_{\ell=0}^{L_2} h_{2,\ell}\ell! \sum_{i=0}^{\ell} \frac{1}{(\ell-i)!} [\tau_1^{\ell-i} E_{i+3}(\tau_1 - \tau) - \tau_2^{\ell-i} E_{i+3}(\tau_2 - \tau)] + \frac{\omega_1}{4\pi} \rho_1 \sum_{n=0}^{K_1} a_{1,n} n! \Bigg[(-1)^{n+1} E_{n+3}(2\tau_1 - \tau) \\
& + \sum_{i=0}^{n} \frac{(-1)^i \tau_1^{n-i}}{(n-i)!} E_{i+3}(\tau_1 - \tau) \Bigg] + \frac{\omega_2}{4\pi} \Gamma_2 \sum_{n=0}^{K_2} a_{2,n} n! \sum_{i=0}^{n} \frac{1}{(n-i)!} [\tau_1^{n-i} E_{i+3}(\tau_1 - \tau) - \tau_2^{n-i} E_{i+3}(\tau_2 - \tau)]
\end{aligned} \tag{B1}
$$

$$
\begin{aligned}
I_2(\tau) = {} & \Gamma_1 \theta_L^4 E_3(\tau) + \rho_2 \theta_R^4 E_3(\tau_2 + \tau - 2\tau_1) + \Gamma_1 \sum_{\ell=0}^{L_1} h_{1,\ell}\ell! \left[(-1)^{\ell+1} E_{\ell+3}(\tau) + \sum_{i=0}^{\ell} \frac{(-1)^i \tau_1^{\ell-i}}{(\ell-i)!} E_{i+3}(\tau - \tau_1) \right] \\
& + \rho_2 \sum_{\ell=0}^{L_2} h_{2,\ell}\ell! \sum_{i=0}^{\ell} \frac{1}{(\ell-i)!} [\tau_1^{\ell-i} E_{i+3}(\tau - \tau_1) - \tau_2^{\ell-i} E_{i+3}(\tau + \tau_2 - 2\tau_1)] + \frac{\omega_1}{4\pi} \Gamma_1 \sum_{n=0}^{K_1} a_{1,n} n! \Bigg[(-1)^{n+1} E_{n+3}(\tau) \\
& + \sum_{i=0}^{n} \frac{(-1)^i \tau_1^{n-i}}{(n-i)!} E_{i+3}(\tau - \tau_1) \Bigg] + \frac{\omega_2}{4\pi} \rho_2 \sum_{n=0}^{K_2} a_{2,n} n! \sum_{i=0}^{n} \frac{1}{(n-i)!} [\tau_1^{n-i} E_{i+3}(\tau - \tau_1) - \tau_2^{n-i} E_{i+3}(\tau + \tau_2 - 2\tau_1)]
\end{aligned} \tag{B2}
$$

Acknowledgment

The support of this work from NATO Grant 85/0334 is gratefully acknowledged.

References

[1]Viskanta, R., "Heat Transfer by Conduction and Radiation in Absorbing and Scattering Materials," *Journal of Heat Transfer*, Vol. 87, 1965, pp. 143-150.

[2]Özisik, M. N. and Lii, C. C., "Transient Radiation and Conduction in an Absorbing, Emitting, and Scattering Slab with Reflective Boundaries," *International Journal of Heat and Mass Transfer*, Vol. 15, 1972, pp. 1175-1179.

[3]Ratzel, A. C. and Howell, J. R., "Heat Transfer by Conduction and Radiation in One Dimensional Planar Media Using the Differential Approximation," *Journal of Heat Transfer*, Vol. 104, 1982, pp. 388-391.

[4]Al Abed, A. and Sacadura, J. F., "A Monte Carlo-Finite Difference Method for Coupled Radiation-Conduction Heat Transfer in Semitransparent Media," *Journal of Heat Transfer*, Vol. 105, 1983, pp. 931-933.

[5]Sutton, W. H., "A Short Time Solution for Coupled Conduction and Radiation in a Participating Slab Geometry," ASME Paper 84-HT-34, 1984.

[6]Crosbie, A. L. and Viskanta, R., "Interaction of Heat Transfer by Conduction and Radiation in a Nongray Planar Medium," *Warme- und Stoffubertragung*, Vol. 4, 1971, pp. 205-212.

[7]Özisik, M. N. and Shouman, S. M., "Source Function Expansion Method for Radiative Transfer in a Two-Layer Slab," *Journal of Quantitative Spectroscopy Radiative Transfer*, Vol. 24, 1980, pp. 441-449.

[8]Özisik, M. N. and Shouman, S. M., "Radiative Transfer in an Isotropically Scattering Two-Region Slab with Reflecting Boundaries," *Journal of Quantitative Spectroscopy Radiative Transfer*, Vol. 26, 1981, pp. 1-9.

[9]Özisik, M. N., *Radiative Transfer*, John Wiley and Sons, New York, 1973.

[10]Özisik, M. N. and Yener, Y., "The Galerkin Method for Solving Radiation Transfer in Plane-Parallel Participating Media," *Journal of Heat Transfer*, Vol. 104, 1982, pp. 351-354.